

Preferential Enrichment of Chemistry at Polymer Surfaces

LEONARDO C. LOPEZ and DAVID W. DWIGHT,* *Center for Adhesion Science and Department of Materials Engineering, Virginia Polytechnic Institute and State University, Blacksburg, Virginia 24061*

Synopsis

The preferential enrichment of specific chemical groups that occur at the surface of three classes of polymers was studied by means of X-ray photoelectron spectroscopy (XPS or ESCA). The material variables included bulk chemical composition, degree of crystallinity, and crosslinking. It was found that XPS is capable of detecting PET cyclic oligomers that were forced to the surface during crystallization. A new PET surface texture was observed by SEM on PET surfaces from which the oligomer crystals were extracted. A crystalline 1:1 alternating copolymer of ethylene/chlorotrifluoroethylene presented a preferential arrangement of ethylene segments closer to the surface relative to the chlorotrifluoroethylene groups. A small amount of contamination strongly affected that surface composition. In linear segmented polyurethanes, enrichment of the surfaces with soft segments occurred. However, this segregation seemed inhibited by crosslinking.

INTRODUCTION

The interaction of a polymer with its surroundings occurs at the surface. Many of the properties of polymers depend upon the surface composition and structure. Moreover, the surface properties of solids are essential in many applications such as adhesion,¹ corrosion,² bio-implants,³⁻⁵ friction and wear.⁶ Consequently, knowledge of the chemical composition and gradients in the outermost atom layers is of basic importance for the understanding and prediction of surface properties. Several spectroscopic techniques such as X-ray photoelectron spectroscopy (XPS or ESCA), secondary ion mass spectroscopy (SIMS), ion scattering spectroscopy (ISS), and Fourier transformed infrared-internal reflection spectroscopy (FTIR-IRS) have been utilized to characterize surfaces. Of these, XPS seems to be the most widely used due to its versatility and comparative ease of data interpretation.⁷⁻⁹

XPS involves the irradiation of a sample with x-rays and determination of the energy and number of electrons emitted from the sample. The kinetic energy of the emitted electrons depends on the atomic environment, the energy of the incident X-ray beam, and the spectrometer work function. These variables are related through

$$KE = h\nu - BE - \varphi \quad (1)$$

*To whom correspondence should be addressed. Current address: Dwight Associates, P.O. Box 160, Sumneytown, PA 18084.

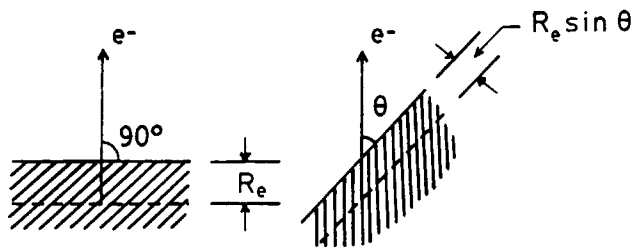


Fig. 1. Mechanism for the enhancement of surface sensitivity.

where $h\nu$ is the photon energy, BE is the binding energy of the atomic orbital from which the electron is ejected, and ϕ is the work function correction.⁸ An important characteristic of XPS is that in solids the photoelectrons can only escape from a very short distance underneath the surface.⁹ Therefore, the technique provides information about the chemical composition of the outermost layers of the specimen. This surface sensitivity can be enhanced by angular dependent depth profiling (XPS(θ)).¹⁰⁻¹² This technique involves changing the angle between the surface of the sample and the electron analyzer slit. As shown in Figure 1, the analysis depth is proportional to the photoelectron exit angle.

XPS has been utilized for the analysis of commercially available segmented polyurethanes such as Avcothane,^{13,14} Biomer,^{13,15} Tygothane, Superthane, and Pellethane.¹⁶ In all cases, an enrichment of the surface with one of the components was found. Avcothane, a polyether urethane containing 10% by weight of poly(dimethyl siloxane) (PDMS), was found to have the surface covered by PDMS.^{13,14} Biomer, a polyether urethane, presented enrichment with soft segments at the air-polymer interface.^{13,15} Similar results were observed on Tygothane, Superthane, and Pellethane.¹⁶ However, the results obtained for these three polymers were precluded, presumably, by a long-chain fatty acid amide present at the polymer surfaces. Knutson and Lyman^{17,18} examined the effect of molecular weight of the soft segment on the composition at the surface of block copolyether-urethane-ureas using XPS and FTIR. These authors studied polymers synthesized from polypropylene glycol with various molecular weights (700, 1000 and 2000), methylene bis(4-phenylisocyanate), and ethylene diamine. An enrichment of the surface with the polyether soft segments was found at the three molecular weights. However, polyurethanes containing soft segments with MW = 700, 1000 showed higher concentration of ether segments at the surface than those having soft segments with MW = 2000.

Graft and block copolymers also have been the subject of surface analysis by means of XPS. Thomas and O'Malley used XPS(θ) to study the surface composition of polystyrene (PS)/poly(ethylene oxide) (PEO) diblock¹⁹ and triblock²⁰ copolymers. The surface composition of the copolymers was found to be higher in PS than the bulk composition. Clark et al.²¹ investigated the surface morphology of AB block copolymers of PDMS/PS containing 23% and 59% weight of PS. The XPS data indicated a surface overlayer of PDMS in both polymers. Thomas and O'Malley²² also found enrichment of the surface with PDMS in random block copolymers of PDMS with poly(hexa-

methylene sebacate). McGrath et al.,²³ Dwight and co-workers²⁴ and Riffle²⁵ examined perfectly alternating block copolymers of poly(bisphenol-A-carbonate) (PC)/PDMS and PC/polysulfone (PSF) with the help of XPS. In both cases, the lower surface free energy component dominated the surface; i.e., PDMS in the PC/PDMS copolymer and PC in the PC/PSF system. Similar results were found in block copolymers of PDMS with poly(ether urethane) Estane,²⁶ poly(bisphenol-A-sulfone), poly(aryl ester), polyurea, and polyimide.²⁷ The lower surface energy component PDMS dominated the surface in all cases. López et al.²⁸ studied liquid crystalline copolyesters by means of XPS(θ). Shake-up satellites were utilized for the characterization. It was observed that copolyesters containing aromatic and cycloaliphatic blocks presented surface enrichment by the cycloaliphatic blocks.

In our continuing research on structure/property relationships at polymer surfaces, we discovered unusual effects related to composition and bonding that were unique in polyesters, ethylene/chlorotrifluoroethylene copolymers, and polyurethanes. The present study reports some details of the analysis of examples from those three classes of polymeric materials by means of XPS(θ).

EXPERIMENTAL

The materials used in this investigation were as follows:

1. Poly(ethylene terephthalate) (PET) film supplied by E. I. du Pont de Nemours and Co., Newark, DE.

2. Polychlorotrifluoroethylene (PCTFE) powder provided by 3M Co., St. Paul, MN, and 1 : 1 alternating copolymer of ethylene/chlorotrifluoroethylene (E/CTFE) powder obtained from Scientific Polymer Products, Ontario, NY. Additional samples of both PCTFE and E/CTFE were supplied by Allied Corp., Morristown, NJ.

3. Ester Estane [31% MDI, 69% poly(tetramethylene adipate), TMAD, MW = 2000] and ether Estane (35% MDI, 65% PTMO MW = 1000) obtained from B. F. Goodrich Co., Chemical Group, Cleveland, OH.

4. Solithane-based polyurethane from Thiokol/Chemical Division, Trenton, NJ. This polyurethane consists of a low molecular weight triisocyanate polymerized with a polyol (29% by weight) and crosslinked with triisopropanolamine (5% by weight).

The PET films were crystallized in a vacuum oven to 22, 29, 39, and 51% crystallinity following the methods of Tant and Wilkes.²⁹ PCTFE and E/CTFE films were compression-molded between aluminum foils at 260°C for 10 min. Ester and ether Estanes were solution-cast from tetrahydrofuran directly onto the analysis probe. The Solithane-based polyurethane was polymerized directly on the analysis probe. Bulk samples of the polyurethanes were fresh surfaces created by slicing a sample with a new blade immediately prior to introduction into the analysis chamber. This sample preparation method, however, creates a new surface that might undergo polymer chain rearrangement to minimize surface energy.

A Kratos XSAM 800 X-ray photoelectron spectrometer was utilized with a hemispherical electron analyzer and a MgK $\alpha_{1,2}$ source. The measured full width at half maximum (FWHM) for a poly(dimethyl siloxane) standard was 1.8 eV. Gaussian peaks of 1.8 eV FWHM were assumed in a least squares

curve fitting routine. Nonlinear background subtraction was performed previous to curve fitting. The angular dependent depth profiling was performed by rotating the sample probe and changing the angle between the surface of the sample and the electron analyzer.¹⁰⁻¹² All the specimens utilized for angular dependent studies were verified as microscopically smooth by scanning electron microscopy. Photomicrographs were obtained with a JEOL Model 35C scanning electron microscope (SEM).

RESULTS AND DISCUSSION

Poly(ethylene Terephthalate)

Figure 2 presents the carbon 1s spectra of PET for different degrees of crystallinity as well as a 51% crystalline sample after chloroform extraction. Curve-fitting illustrated in Figure 3 brings out components of the C_{1s} envelope located at BE = 285.0 eV assigned to C—C and C—H, at BE = 286.6 eV assigned to C—O, and at BE = 289.0 eV corresponding to C=O of the ester group. Similarly, the O_{1s} spectrum shows components located at BE = 532.1 eV corresponding to O=C and at BE = 533.7 eV assigned to O—C.

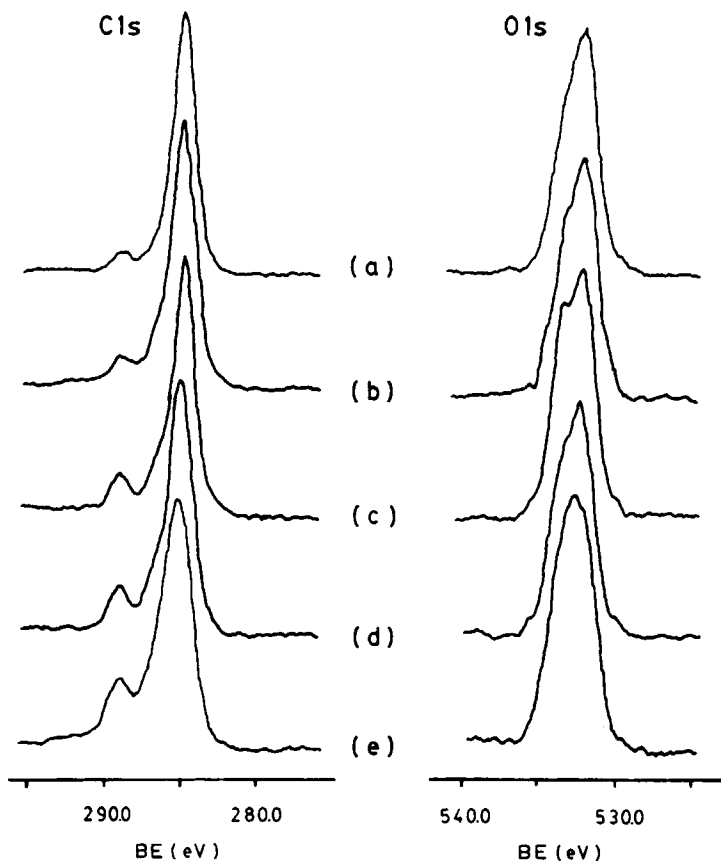


Fig. 2. High resolution C_{1s} and O_{1s} spectra of PET of (a) 22%, (b) 29%, (c) 39%, (d) 51% crystallinities, and (e) 51% crystallinity after chloroform extraction.

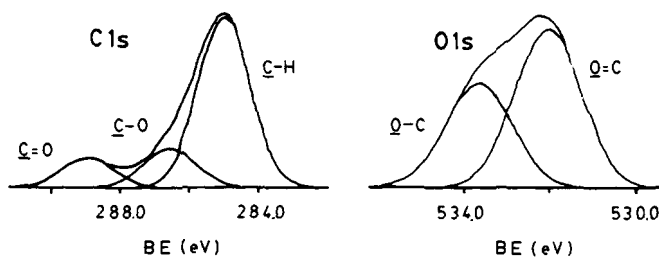


Fig. 3. Computer curve-fitted C_{1s} and O_{1s} XPS spectra of PET showing the different component peaks. A 1.8-eV full width at half-height was utilized.

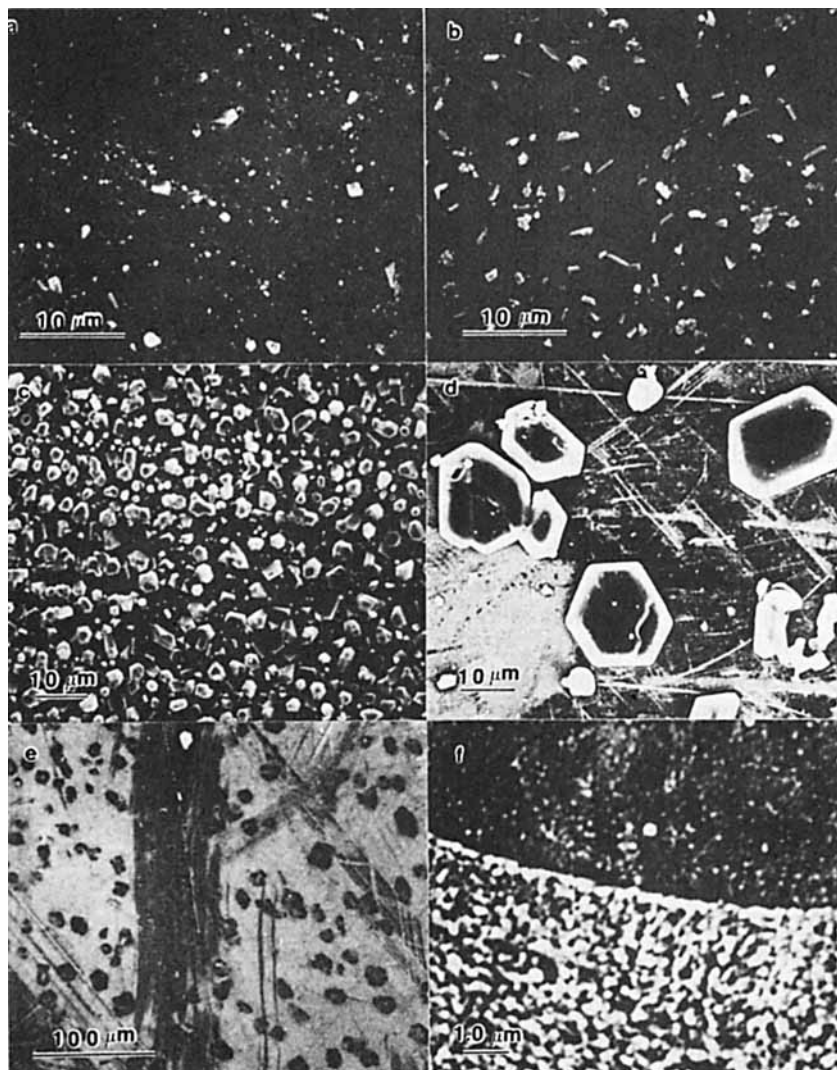


Fig. 4. SEM micrographs of PET of (a) 22%, (b) 29%, (c) 39%, and (d) 51% crystallinities showing the presence of cyclic oligomers at the surface. (e) and (f) PET 51% crystallinity after chloroform extraction.

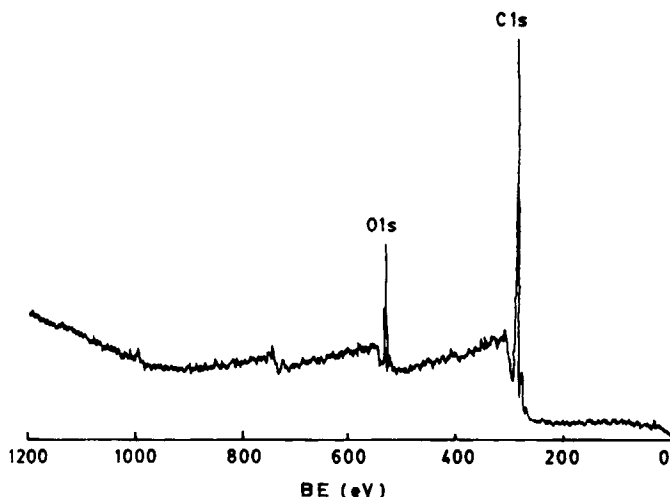


Fig. 5. Low resolution XPS spectrum of PET 51% crystalline showing no contamination.

Comparison of the O_{1s} peak shapes with spectra from the literature³⁰ reveals a discrepancy. The O_{1s} spectra collected in the present study show an $\underline{O=C/O}-C$ ratio greater than unity, whereas a 1:1 ratio is expected from stoichiometry as observed by Dwight et al.³⁰ However, the O/C ratio (3.7) does not indicate oxidation of the polymer surface. In addition, the $\underline{O=C/O}-C$ ratio discrepancy cannot be attributed to contamination, since a wide scan of a 51% crystalline PET sample does not show any contamination (see Fig. 5).

Further characterization by scanning electron microscopy revealed particles apparently crystallized on the surface, which we believe are cyclic oligomers^{31,32} [Figs. 4(a)–(d)]. The volume of the crystals increases in proportion to the degree of crystallinity in the bulk. Diffusion of the cyclic oligomers towards the surface of PET must take place during annealing.

Although these cyclic oligomers have been studied by microscopy,^{31,32} they were not known to alter the XPS spectra of PET. Chloroform extraction of the 51% crystalline sample removed the hexagonal crystals from the surface, leaving depressions that have a different texture [Fig. 4(e), (f)]. The XPS spectra after extraction closely resembles those in the literature; i.e., there is a 1:1 ratio of the oxygen peak components. Therefore, XPS is capable of detecting these cyclic oligomers when they are present at the PET surface.

Halogen-Containing Polymers

The results in this section depended upon the source of the polymer. Figure 6 depicts a typical low resolution spectrum corresponding to a PCTFE sample that shows a small O_{1s} peak corresponding to contamination. Also, the characteristic F_{1s} , C_{1s} , Cl_{2p} , F_{2s} , and F_{Auger} peaks are observed. Figure 7 presents high resolution spectra for PCTFE and 1:1 alternating E/CTFE copolymer that were free of contamination. In the computer curve-fitted C_{1s} spectra, PCTFE has two components located at BE = 290.4 eV assigned to \underline{CFCl} and at BE = 291.6 eV assigned to \underline{CF}_2 . The copolymer shows four

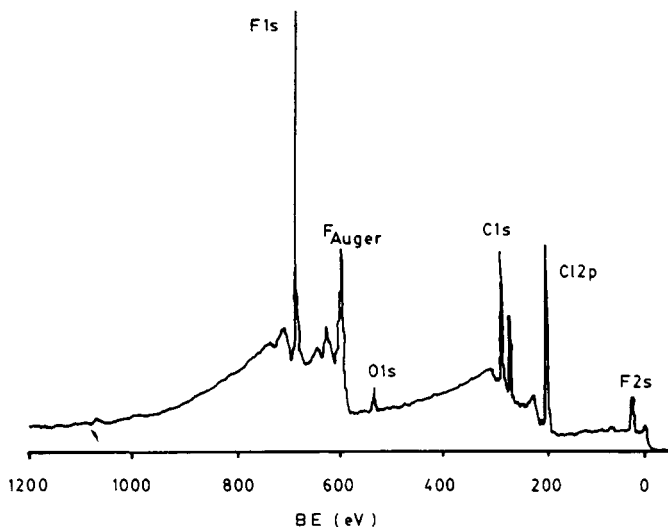


Fig. 6. Low resolution XPS spectrum of commercial grade PCTFE. Note the small oxygen contamination peak.

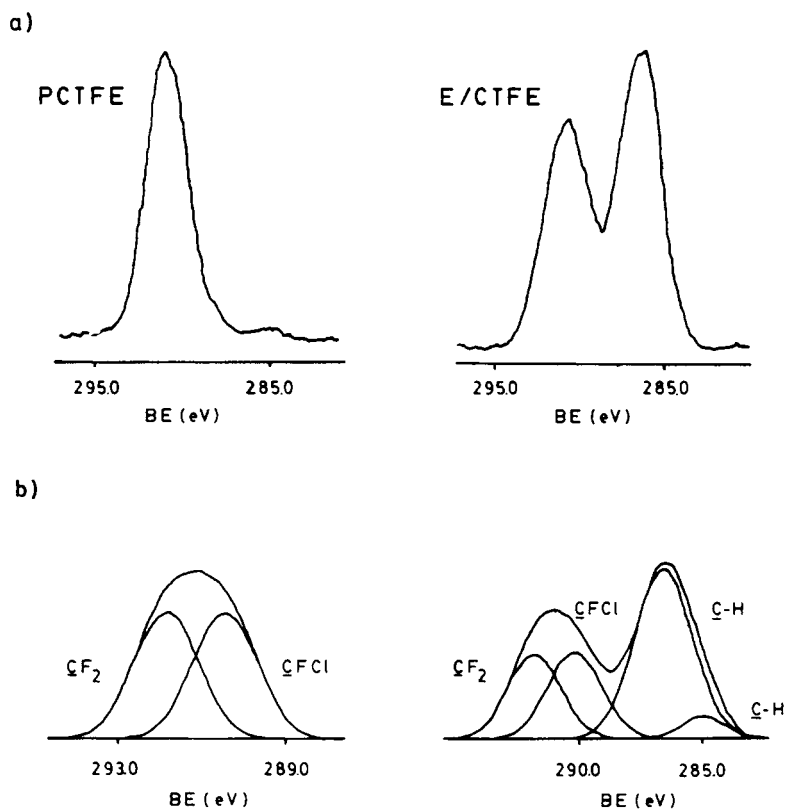


Fig. 7. (a) High resolution C_{1s} spectra of PCTFE and 1:1 alternating E/CTFE copolymer. (b) Computer curve-fitted spectra showing the different component peaks. A 1.8-eV peak width at half-maximum was utilized for the curve fitting.

components located at BE = 290.3 eV corresponding to $\underline{\text{C}}\text{FCl}$, at BE = 291.6 eV assigned to $\underline{\text{C}}\text{F}_2$, at BE = 286.5 eV due to $\underline{\text{C}}\text{H}_2$, and at BE = 285.0 eV possibly corresponding to carbonaceous contamination, or to a less than perfect alternating copolymer. As will be shown in the case of PCTFE, there was no contamination on the samples. Therefore, it is our belief that this component is due to a less than perfect alternating copolymer with some CH_2 sequences longer than two. The 1.5 eV shift of the $\underline{\text{C}}-\text{H}$ component in the copolymer is due to secondary fluorine chemical shift effects produced by the CTFE units adjacent to the ethylene units. This energy shift is in excellent agreement with the work of Clark,³³ who determined many of the secondary effects on the chemical shifts in polymers.

The F_{1s} high resolution spectra, centered at BE = 689.0 eV for both PCTFE and E/CTFE were identical. A single peak was observed with full width at half maximum of 1.9 eV. The two components corresponding to $\underline{\text{F}}-\text{C}-\text{F}$ and $\underline{\text{F}}-\text{C}-\text{Cl}$ groups separated 0.1 eV could not be resolved. As noted by Clark,³³ the energy separation of these two components is in the edge of resolution of the energy scale. The Cl_{2p} spectra also were identical for both

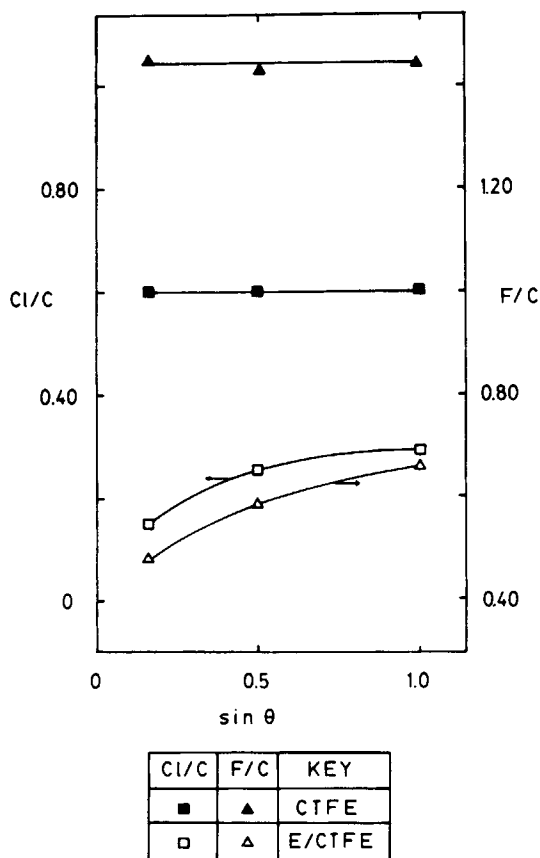


Fig. 8. Plots of $\text{F}_{1s}/\text{C}_{1s}$ and $\text{Cl}_{2p}/\text{C}_{1s}$ intensity ratios vs. $\sin \theta$ for pure PCTFE and 1:1 alternating E/CTFE copolymer.

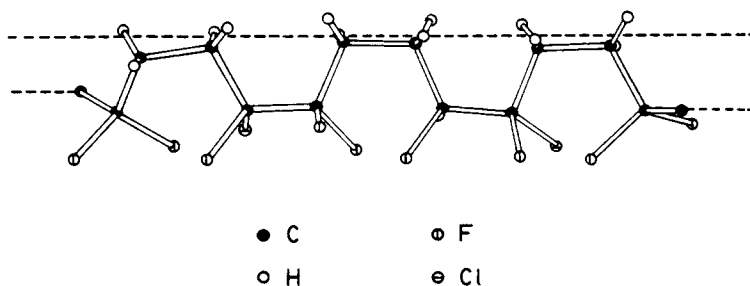


Fig. 9. Schematic representation of the atomic arrangement on the surface of an E/CTFE 1 : 1 alternating copolymer.

polymers, showing the $2p_{3/2}$ component at BE = 200.5 eV and the $2p_{1/2}$ at BE = 202.1 eV.

Figure 8 shows the F_{1s}/C_{1s} and Cl_{2p}/C_{1s} intensity ratios vs. electron exit angle for PCTFE and E/CTFE. For the pure PCTFE both ratios remain constant, indicating a homogeneous uncontaminated polymer surface. How-

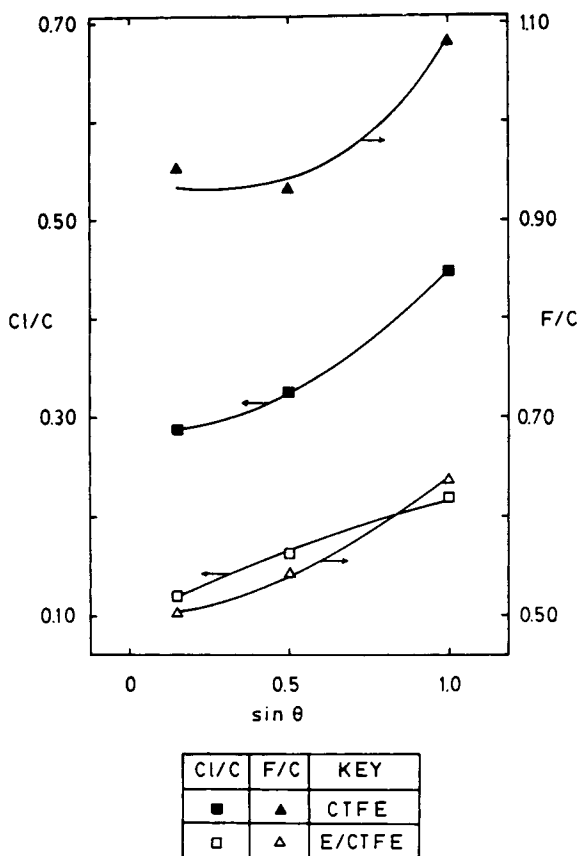


Fig. 10. Plots of F_{1s}/C_{1s} and Cl_{2p}/C_{1s} intensity ratios versus $\sin \theta$ for commercial grade samples of PCTFE and 1 : 1 alternating E/CTFE copolymer.

ever, in pure E/CTFE copolymer, both ratios decrease as we approach the surface. As expressed before, the C_{1s} component located at $BE = 285$ eV of E/CTFE may be due to a less than perfect alternating copolymer; i.e., the copolymer has some CH_2 sequences longer than two units. This effect would contribute to the lowering of the F_{1s}/C_{1s} and Cl_{2p}/C_{1s} ratios. However, in Figure 8 the component corresponding to $BE = 285.0$ eV was subtracted to perform the calculations. Consequently, the data suggest the preferential arrangement of ethylene units closer to the surface relative to CTFE groups. Based on these observations, a simplified schematic representation of the atomic ordering at the surface of the copolymer may be pictured, as shown in Figure 9. The critical surface tensions of homopolymers PE (28 dyn/cm) and PCTFE (31 dyn/cm) would lead to the prediction of preferential surface segregation of PE in blends or block copolymers. Our new results with alternating copolymers indicate that similar enrichment effects occur. However, if CH_2 sequences longer than two are present, the schematic representation in Figure 9 must include $(CH_2)_{2+n}$ sequences that would be partially located at the surface of the polymer. Figure 9 does not imply that the polymer is 100% crystalline, or that the surface is 100% crystalline. Indeed, a semicrystalline polymer will present amorphous regions at the surface. However, these regions do not need to be absolutely disordered since amorphous polymers can also present some degree of local ordering without forming crystalline entities.

Figure 10 presents angle dependent XPS data for the PCTFE and E/CTFE specimens that showed a small oxygen contamination peak (see Fig. 6). The F_{1s}/C_{1s} and Cl_{2p}/C_{1s} ratios corresponding to contaminated PCTFE are lower than those of pure PCTFE. In addition, these ratios decrease as the polymer surface is approached, indicating a heterogeneous surface composition. This can only be explained in terms of a small concentration of contamination affecting the chemical composition and atomic arrangement at the surface of

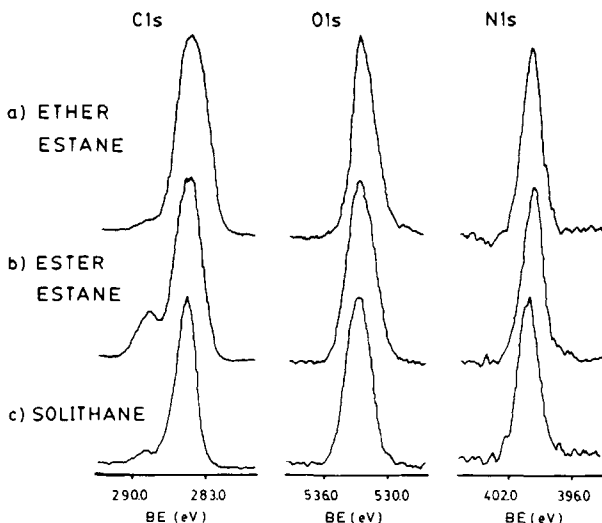


Fig. 11. High resolution C_{1s} , O_{1s} , and N_{1s} spectra of (a) ether Estane, (b) ester Estane, and (c) Solithane-based polyurethanes.

the polymer. Such gradients in surface chemical composition would not be detected in bulk analyses, but might play a major role in determining surface properties.

Polyurethanes

Figure 11 shows C_{1s} , O_{1s} and N_{1s} high resolution spectra corresponding to the three polyurethanes studied, and Figure 12 presents the C_{1s} and O_{1s} computer curve-fitted peaks. The C_{1s} envelope has three components located at BE = 285.0 eV, corresponding to the superposition of $\underline{C}-H$, $C-C$, and $\underline{C}-N$ contributions, BE = 286.5 eV assigned to $\underline{C}-O$ species in ether and ester groups, and BE = 289.1 eV corresponding to $\underline{C}=O$ overlap from carbamate (urethane) and ester groups. The O_{1s} peaks show two components located at BE = 531.9 eV assigned to $\underline{O}=C$ and at BE = 533.5 eV corresponding to $\underline{O}-C$. The curve-fitted spectra also bring out the different intensities of the C_{1s} and O_{1s} peaks for the polyurethanes. Ether Estane

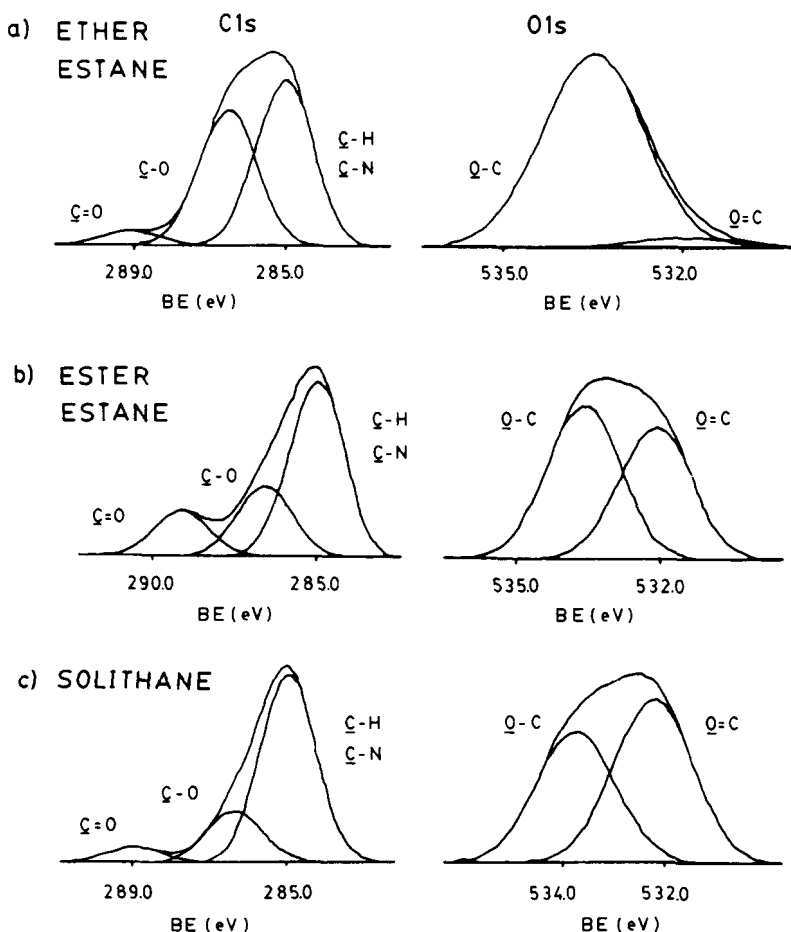


Fig. 12. C_{1s} and O_{1s} computer curve-fitted spectra of (a) ether Estane, (b) ester Estane, and (c) Solithane-based polyurethanes showing the different component peaks. A 1.8-eV peak width at half-maximum was utilized for the curve fitting.

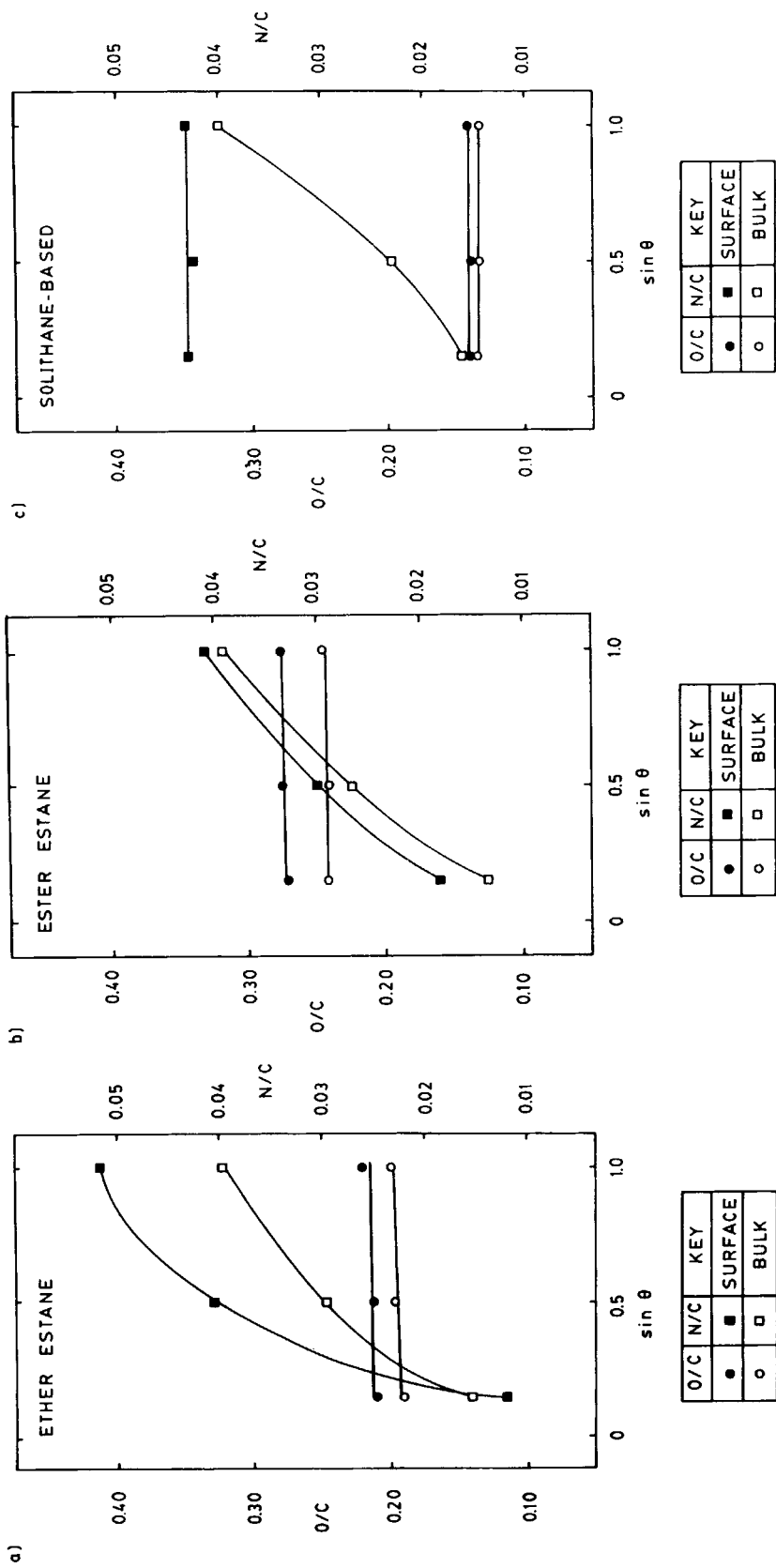


Fig. 13. Plots of O_{1s}/C_{1s} and N_{1s}/C_{1s} intensity ratios vs. $\sin \theta$ for (a) ether Estane, (b) ester Estane, and (c) Solithane-based polyurethanes.

presents the lowest intensity $\text{C}=\text{O}$ component and the highest $\text{C}-\text{O}$ component, consistent with high concentration of ether soft segments. On the other hand, ester Estane has the highest relative intensity $\text{C}=\text{O}$ component due to the presence of the tetramethylene adipate soft segments. Solithane-based polyurethane shows a $\text{C}=\text{O}$ component of intermediate intensity, providing some insight upon the chemical composition of these proprietary material. The O_{1s} spectra show corresponding trends.

Figure 13a-c presents the angular dependent XPS data corresponding to "bulk" and "surface" specimens of the polyurethanes. The depth profiles of "surface" specimens of ether and ester Estane show constant $\text{O}_{1s}/\text{C}_{1s}$ ratios and decreasing $\text{N}_{1s}/\text{C}_{1s}$ ratios as the surface is approached. This indicates a depletion of nitrogen-containing (hard segments) species from the surface. The surface is enriched with soft segments. These results are in agreement with studies performed on other polyurethanes by Ratner.¹⁶ Similar results are also found in the "bulk" specimens of these two polyurethanes. However, the sample preparation method may induce changes in the polymer chain arrangement to reduce surface energy.

The "surface" specimen of the crosslinked Solithane-based polyurethane presents both $\text{O}_{1s}/\text{C}_{1s}$ and $\text{N}_{1s}/\text{C}_{1s}$ ratios constant at different electron exit angles. This indicates a homogeneous surface composition. This is consistent with the investigations of Ophir and Wilkes³⁴ that indicated that the extent of domain formation (phase separation) in polyurethanes is decreased by an increase in crosslink density. However, the bulk specimens present constant $\text{O}_{1s}/\text{C}_{1s}$ ratio and decreasing $\text{N}_{1s}/\text{C}_{1s}$ ratio as the outermost layers are approached. This suggests a depletion of hard segments from the surface. One explanation for this is that the slicing procedure used to prepare "bulk" samples produces bond breaking and heating due to friction of the blade. Since the soft segments are above their glass transition temperature, rearrangement of these polymer segments may occur rather quickly. Therefore, this could result in a preferential reorientation of the soft segments towards the surface to reduce surface energy. In addition, the blade friction can produce some transfer of soft segment towards the surface of the cut resulting in the heterogeneous chemical composition observed.

CONCLUSIONS

X-ray photoelectron spectroscopy is capable of detecting PET oligomers forced to the surface during crystallization. Therefore, the determination of the degree of crystallinity of polymer thin films may be possible by including a "label" that blooms to the surface in proportion to the crystallinity. Then, the label may be quantified by XPS and correlated with the degree of crystallinity. A new PET surface texture is apparent on PET surfaces from which oligomer crystals are extracted. Thus, controlled surface topographic modification can be obtained by blending-in species that migrate to the surface and subsequently can be extracted by a solvent.

Ethylene/chlorotrifluoroethylene alternating copolymer shows a preferential surface conformation with the ethylene groups closer to the surface and the CTFE units oriented towards the bulk of the polymer. A small amount of contamination had a profound effect on the chemical composition gradient at

CTFE and E/CTFE surfaces. This shows the value of XPS in the analysis of commercial polymers, where the actual surface composition is likely to be an important, unknown variable.

Crosslinking can inhibit the soft segment segregation that occurs in linear segmented polyurethanes. Consequently, crosslinking can be regarded as a means to "lock" chemical groups at the surface of the polymer.

The financial support of the Office of Navy Research (ONR) is gratefully acknowledged. Thanks are also due to the referee for helpful comments.

References

1. D. F. Kagan, V. V. Prokopenko, V. M. Malinskii, and N. F. Bakeyev, *Polym. Sci. U.S.S.R.*, **32**, 124 (1972).
2. J. Schultz, K. C. Sehgal, and M. E. R. Shanahan, *Adhesion 1*, K. W. Allen, Ed., Applied Science, London, 1977, p. 269.
3. R. E. Baier, V. R. E. Baier, V. L. Gott, and A. Feruse, *Trans. Am. Soc. Artif. Int. Organs*, **16**, 50 (1970).
4. D. J. Lyman, L. C. Metcalf, D. Albo, Jr., K. F. Richards, and J. Lamb, *Trans. Am. Soc. Artif. Organs*, **20B**, 474 (1974).
5. D. J. Lyman, K. Knutson, B. McNeil, and K. Shibatani, *Trans. Am. Soc. Artif. Organs*, **21**, 49 (1975).
6. M. J. Owens and J. Thompson, *Br. Polym. J.*, **4**, 297 (1972).
7. K. Siegbahn et al., ESCA-Atomic, *Molecular and Solid State Structure Studied by Means of Electron Spectroscopy*, Nova. Act. Regiae, Soc. Sci. Upsaliensis, Ser. IV, North-Holland, Amsterdam-London, 1967, Vol. 20.
8. D. T. Clark, in *Handbook of X-ray and Ultraviolet Photoelectron Spectroscopy*, D. Briggs, Ed., Heyden and Son, London, 1978, p. 211.
9. D. Briggs, in *Electron Spectroscopy: Theory, Techniques and Applications*, C. R. Brundle and A. D. Baker, Eds., Academic, New York, 1979, Vol. 3, p. 306.
10. (a) C. S. Fadley and S. A. L. Bergstrom, *Phys. Lett.* **35A**, 375 (1971); (b) C. S. Fadley and S. A. L. Bergstrom, in *Electron Spectroscopy*, D. A. Shirley, Ed., North-Holland, Amsterdam, 1972, p. 233.
11. W. A. Fraser, J. V. Florio, W. N. Delgass, and W. D. Robertson, *Surf. Sci.*, **36**, 661 (1973).
12. C. S. Fadley, in *Electron Spectroscopy: Theory, Techniques and Applications*, C. S. Brundle and A. D. Baker, Eds., Academic, London, 1978, Vol. 2, p. 1.
13. C. S. Paik Sung and C. B. Hu, *J. Biomed. Mater. Res.*, **13**, 161 (1979).
14. S. W. Graham and D. M. Hercules, *J. Biomed. Mater. Res.*, **15**, 349 (1981).
15. S. W. Graham and D. M. Hercules, *J. Biomed. Mater. Res.*, **15**, 465 (1981).
16. B. D. Ratner, in *Photon, Electron and Ion Probes of Polymeric Structure and Properties*, D. W. Dwight, T. J. Fabish, and H. R. Thomas, Eds., ACS Symp. Ser. No. 162, Am. Chem. Soc., Washington, DC, 1981, p. 371.
17. K. Knutson and D. J. Lyman, *Org. Coat. Plast. Chem.*, **42**, 621 (1980).
18. K. Knutson and D. J. Lyman, *Polym. Sci. Technol.*, **14**, 173 (1981).
19. H. R. Thomas and J. J. O'Malley, *Macromolecules*, **12**, 323 (1979).
20. J. J. O'Malley, H. R. Thomas, and G. M. Lee, *Macromolecules*, **12**, 996 (1979).
21. D. T. Clark, J. Peeling, and J. M. O'Malley, *J. Polym. Sci., Polym. Chem. Ed.*, **14**, 543 (1976).
22. H. R. Thomas and J. J. O'Malley, in *Photon, Electron and Ion Probes of Polymer Structure and Properties*, D. W. Dwight, T. J. Fabish, and H. R. Thomas, Eds., ACS Symp. Ser. 162, Am. Chem. Soc., Washington, DC, 1981, p. 319.
23. J. E. McGrath, D. W. Dwight, J. S. Riffle, T. F. Davidson, D. C. Webster, and R. Viswanathan, *Polym. Prepr.*, **20**(2), 528 (1979).
24. D. W. Dwight, J. E. McGrath, A. R. Beck, and J. S. Riffle, *Polym. Prepr.*, **20**(1), 702 (1979).
25. J. S. Riffle, Ph.D. dissertation, Virginia Polytechnic Institute and State University, Blacksburg, 1980.
26. A. K. Sha'aban, S. McCartney, N. Patel, I. Yilgor, J. S. Riffle, D. W. Dwight, and J. E. McGrath, *Polym. Prepr.*, **24**(2), 130 (1983).

27. N. Patel, M.S. thesis, Virginia Polytechnic Institute and State University, Blacksburg, 1984.
28. L. C. López, D. W. Dwight, and M. B. Polk, *Surf. Interf. Anal.*, **9**, 405 (1986).
29. M. R. Tant and G. L. Wilkes, *J. Appl. Polym. Sci.*, **26**, 2813 (1981).
30. D. W. Dwight, J. E. McGrath, and J. P. Wightman, *J. Appl. Polym. Sci., Appl. Polym. Symp.*, **34**, 35 (1978).
31. A. Perovic and P. R. Sundararajan, *Polym. Bull.*, **6**, 277 (1982).
32. R. Giufria, *J. Polym. Sci.*, **49**, 427 (1961).
33. D. T. Clark, in *Advances in Polymer Friction and Wear*, L. H. Lee, Ed., Plenum, New York, 1975, Vol. 5A, p. 241.
34. Z. H. Ophir and G. L. Wilkes, *Adv. Chem. Ser.*, **176**, 53 (1978).

Received May 1, 1987

Accepted December 15, 1987